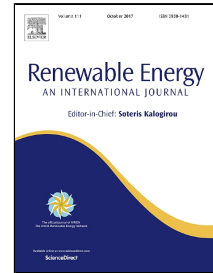


Accepted Manuscript

Influence of Local Geological Data on the Performance of Horizontal Ground-coupled Heat Pump System Integrated with Building Thermal Loads

Chanjuan Han, Kevin M. Ellett, Shawn Naylor, Xiong (Bill) Yu



PII: S0960-1481(17)30526-8
DOI: 10.1016/j.renene.2017.06.025
Reference: RENE 8889
To appear in: *Renewable Energy*
Received Date: 10 November 2016
Revised Date: 26 May 2017
Accepted Date: 04 June 2017

Please cite this article as: Chanjuan Han, Kevin M. Ellett, Shawn Naylor, Xiong (Bill) Yu, Influence of Local Geological Data on the Performance of Horizontal Ground-coupled Heat Pump System Integrated with Building Thermal Loads, *Renewable Energy* (2017), doi: 10.1016/j.renene.2017.06.025

This is a PDF file of an unedited manuscript that has been accepted for publication. As a service to our customers we are providing this early version of the manuscript. The manuscript will undergo copyediting, typesetting, and review of the resulting proof before it is published in its final form. Please note that during the production process errors may be discovered which could affect the content, and all legal disclaimers that apply to the journal pertain.

Influence of Local Geological Data on the Performance of Horizontal Ground-coupled Heat Pump System Integrated with Building Thermal Loads

Chanjuan Han¹, Kevin M. Ellett², Shawn Naylor², Xiong (Bill) Yu^{3*}

¹ Ph.D. Candidate, Department of Civil Engineering, Case Western Reserve University, 2104 Adelbert Road, Bingham Building-Room 203B, Cleveland, OH 44106, cxh432@case.edu.

² Indiana Geological Survey, Indiana University, Bloomington, Indiana 47405, USA.

^{3*} Professor, Department of Civil Engineering, Department of Electrical Engineering and Computer Science (Courtesy Appointment), Department of Mechanical and Aerospace Engineering (Courtesy Appointment), Case Western Reserve University, 2104 Adelbert Road, Bingham Building-Room 206, Cleveland, OH 44106, xy21@case.edu, Corresponding author.

ABSTRACT

Horizontal ground-couple heat pump (GCHP) system incurs lower installation cost compared with the vertical GCHP system. However, the shallow burial depth makes the heat transfer process susceptible to seasonal variations. This paper analyzes the short-term and annual performance of different geothermal heat exchangers' (GHEs) configurations and geological conditions by developing 3D finite element models. Field monitored data of ground temperature and thermal property are incorporated. Six common types of GHE configurations are analyzed, from which the most efficient patterns are identified. The annual performance of optimal GCHP pattern integrated with different types of building loads are analyzed. Major conclusions include (1) application of soil temperature harmonic function as commonly done in the current practice will lead to overestimation of thermal build-up effects underground; (2) utilization of local geological data (i.e., field measured ground temperature and soil thermal properties) helps improve the annual performance of horizontal GCHP system; (3) shift of ground temperature is less significant for GCHP operating in heating dominant areas due to balanced heat injection and extraction. This study indicates incorporating local geological data reduce the GHE design length by 25% to 60% and therefore is a viable strategy to achieve cost effectiveness.

KEYWORDS

Horizontal geothermal heat pump system, finite element model, building thermal load model, building integration, field monitoring data, geology

1. Introduction

The environment issue and fossil fuel crisis have greatly promoted the renewable energy revolution. Geothermal energy, as one type of renewable energy, has been widely explored worldwide. The direct utilization of geothermal energy has been reported to be the most promising renewable energy format, and the total installation capacity at the end of 2014 has increased around 45% compared with that in 2010 [1]. China, United States, Sweden, Turkey and Germany contributed to about 65.8% of the direct-use installed capacity [1]. With the growing awareness and remarkable development of geothermal heat pump system,

37 the application of geothermal energy has opened a promising pathway to achieve sustainability.

38 The most typical and popular utilization of geothermal energy is the ground-coupled heat pump (GCHP)
39 system, which utilizes the geothermal heat exchangers (GHEs) to extract/inject heat from/to the ground.
40 Horizontal GCHP system, whose underground heat exchanger pipes are connected in series or parallel in a
41 horizontal trench, is attractive due to its merits of low installation cost and easy maintenance, particularly for
42 residential applications. Although many numerical [2-8] and experimental [6, 9-12] studies have been
43 conducted to investigate the performance of GCHP system with vertical GHEs over recent years, only limited
44 studies have been reported on GCHP system with horizontal GHEs [13-19]. Congedo et al. [13] conducted
45 a simulation based comparison of GCHP system with horizontal GHEs in three configurations, i.e., linear,
46 helical and slinky. Their results showed that the helical GHE arrangement is the most efficient, and thermal
47 conductivity of the ground is the most influential factor for horizontal GCHP system. Naylor et al. [14]
48 suggested it is necessary to consider the seasonal variations of soil thermal properties to optimize horizontal
49 GCHP system design. Their results indicated using in-situ measured seasonal soil property data can decrease
50 the design length of GHEs by 44-52% compared with applying standard industry practice to the estimate soil
51 thermal properties. Naili et al. [15] carried out an experimental study to characterize the GHEs response and
52 evaluate the optimal parameters of GCHP system with horizontal GHEs installed in a hot climate zone. The
53 highly dependency of horizontal GCHP system on climate and building type in term of economic efficiency
54 was also reported by Wiryadinata [16]. Benli [17] deployed experiments to compare the performance of
55 GCHP system with horizontal and vertical GHEs for a greenhouse heating, which illustrated that although
56 GCHP system with vertical GHEs achieved a higher Coefficient of Performance (COP) than the horizontal
57 counter part, the significant higher installation cost of vertical GHE is a major implementation barrier.
58 Sanaye [18] applied the Genetic Algorithm technique to conduct the thermal and economic simulation and
59 optimization of horizontal GCHP system. Recently, an innovative bio-inspired model that integrated
60 regression techniques and local models was proposed to investigate the ground temperature behavior after
61 installing the horizontal GHEs [19]. Overall, the existing study and knowledge on the behaviors of
62 horizontal GCHP system is limited. Another major problem for GCHP system integration with building is
63 that although many simulation tools (i.e., eQuest, TRNSYS) provide modules to conduct the integrated
64 simulation with the GCHP system, the model of GHE is based on a number of simplifications and ignores the
65 influence of geometry and transient behavior of soil thermal properties, which can be crucial for horizontal
66 GCHP system. These lead to problems (i.e. overdesign) for GCHP system design and operation.

67 This study aims to study the horizontal GCHP system performance with respect to the seasonal variations
68 of the ground conditions. A 3D numerical model is developed to simulate the heat exchange process
69 associated with different horizontal GHE configurations. The seasonal soil parameters from a field
70 monitoring program are used to populate the model parameters, which represent two contrast scenarios, i.e.,
71 one with significant variations of ground thermal properties and one maintains relative stable. The behaviors
72 of horizontal GCHP system in meeting building loads requirements at different climate zones (i.e., seasonal
73 balance, heating dominant, cooling dominant) are analyzed. The study demonstrates the importance of
74 considering the seasonal ground properties variations in improving the design and achieving desired short-
75 term and annual performance of horizontal GCHP system.

76 **2. Numerical Model Development and Implementation**

77 **2.1 Finite Element Modeling**

78 Han and Yu [2] presented a 3D coupled finite element model (FEM) to study the thermal behaviors of
79 vertical GHE and to analyze factors affecting its performance. The model developed in this study refers to

80 the theory described in [2] and therefore is not repeated here to avoid duplication. With this theory, a 3D
 81 FEM was developed for horizontal GHE via a commercial finite element software COMSOL® Multiphysics,
 82 in which, the heat exchange between the fluid and GHE pipe is simulated by non-isothermal pipe flow module
 83 while that between GHE pipe and adjacent ground can be simulated by heat transfer module.

84 In the non-isothermal pipe flow module, the pipe flow is simplified as one-dimensional flow that ignores
 85 the heat transfer in the cross section of fluid inside the pipe (i.e., temperature of the fluid in the cross section
 86 is assumed to be uniform) and improves the computational efficiency. The GHE pipe is assumed to be made
 87 of High-density Polyethylene (HDPE) pipe with an inner diameter of 36 mm and a wall thickness of 2 mm.
 88 In the heat transfer module, the computational domain or the ground is assumed to be a cuboid with dimension
 89 of 35 m (length) × 32 m (width) × 10 m (depth). The GHE pipes are assumed to be installed with the average
 90 depth of 1.5 m below the ground surface. The geometric parameters and material properties are summarized
 91 in Table 1.

92 The Dirichlet boundary condition is applied on the side and bottom boundaries of the computational
 93 domain with magnitude of temperature as a function of depth and time, $T(z,t)$, which can be assigned with
 94 either soil temperatures harmonic function or the in-situ measured soil temperatures. The boundary condition
 95 of heat convection between the ground and atmosphere is described by applying the Robin boundary
 96 condition on the top surface of the ground, where the monitored air temperature is imposed and the
 97 convection coefficient h is assumed to be 0.53 W/m/K according to the literature [20]. In addition, free
 98 tetrahedral mesh method is adopted to generate the tetrahedral elements with the mesh refined near the GHE
 99 pipe to ensure the computational efficiency and accuracy.

100

Table 1. GHE properties

Item	Description
Average installation depth of GHE pipe	1.5 m
Pipe material	HDPE
Pipe diameter D	36 mm
Ground properties	Soil
Fluid in the pipe	Water + 10% ethyl alcohol
Fluid volumetric flow rate Q_v	1 L/s
Ground specific heat capacity $C_{p_{ground}}$	1175 J/kg/K
Fluid thermal conductivity k_{fluid}	0.56 W/m/K
Fluid specific heat capacity $C_{p_{fluid}}$	4190 J/kg/K
Pipe wall (HDPE) thermal conductivity k_{pipe}	0.46 W/m/K

101

Soil temperatures harmonic function

102

103

The soil temperature distribution is estimated as a function of depth and time [21] with associated parameters acquired from Ref. [22], Table.5.11 for Indianapolis, Indiana.

104

$$T(z, t) = T_m + T_a e^{-z \sqrt{\frac{\omega}{2a_s}}} \cos \left[\omega(t - t_0) - z \sqrt{\frac{\omega}{2a_s}} \right] \quad (1)$$

105

106

107

where, T_m is the average ambient temperature at the ground surface, which is set as 12.78°C (55 °F) for Indianapolis. T_a is the amplitude of temperature variation at the ground surface, which is -4.44°C (24 °F). ω is the angular frequency of temperature variations, which is set as $2\pi/365$ d⁻¹. a_s is the solid thermal

108 diffusivity, which is assumed to be $0.8 \times 10^{-6} \text{ m}^2/\text{s}$. t_0 denotes to the time (in days) when the minimum surface
 109 temperature occurs, which is 34 days.

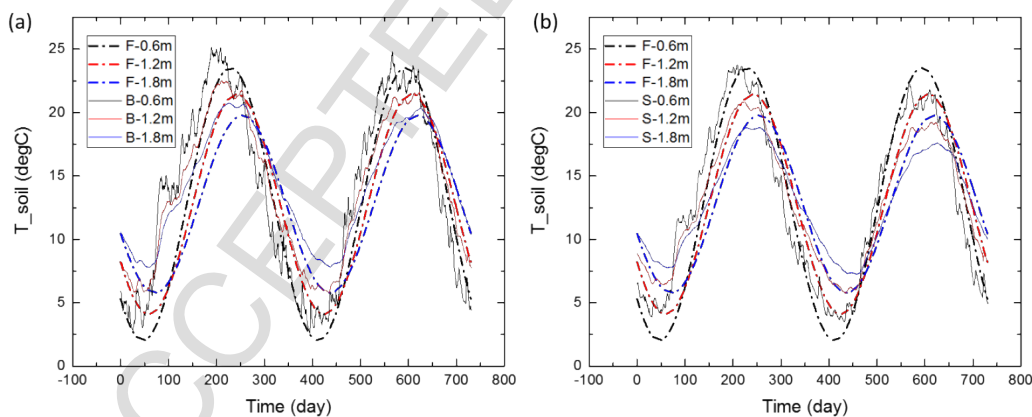
110 The soil temperature profiles at different depth based on Equation (1) are presented in Fig. 1 in dash lines.

111 **In-situ monitored soil temperatures, air temperature, and soil properties**

112 Naylor et al. [14] deployed a shallow monitoring network in Indiana to characterize the dynamic soil
 113 thermal properties under different geological conditions. Total six locations of different hydrogeological
 114 settings and near-surface glacial sediments were monitored. In-situ temperature data was continuously
 115 recorded via the temperature sensors installed at 0.3 m intervals below the ground surface, and in-situ thermal
 116 conductivity and diffusivity were determined via differential temperature sensor aiming to measure radial
 117 differential temperature around a heating wire at 1.2 m depth. The site meteorological data, such as air
 118 temperature, wind speed, relative humidity and precipitation, etc., were also recorded to determine the surface
 119 energy and water budgets, which drive fluxes of energy and moisture in the shallow subsurface.

120 In the study, two sites with/without significant seasonal thermal properties variations are analyzed to
 121 compare the influence of ground soil property variations on the horizontal GCHP system. One site is located
 122 at Bradford Woods with main soil as alluvium, while the other site is at Shelbyville Moraine with main soil
 123 as glacial till.

124 Fig. 1 displays the comparison of the temperature profiles obtained from soil temperature harmonic
 125 function (labeled as F) and in-situ experimentally measured soil temperatures at two sites in the State of
 126 Indiana, USA, i.e., Bradford Woods (labeled as B) and Shelbyville Moraine (labeled as S). The temperature
 127 at the shallow ground shows clear seasonal variations. The ground temperature at certain depth predicted by
 128 the harmonic function shows a similar trend as field monitored data, although they do not exactly match each
 129 other. The amplitude and the corresponding maximum and minimum occurring moments are somehow
 130 consistent, indicating the application of the soil temperature harmonic function is acceptable with proper
 131 calibrations to certain extent.

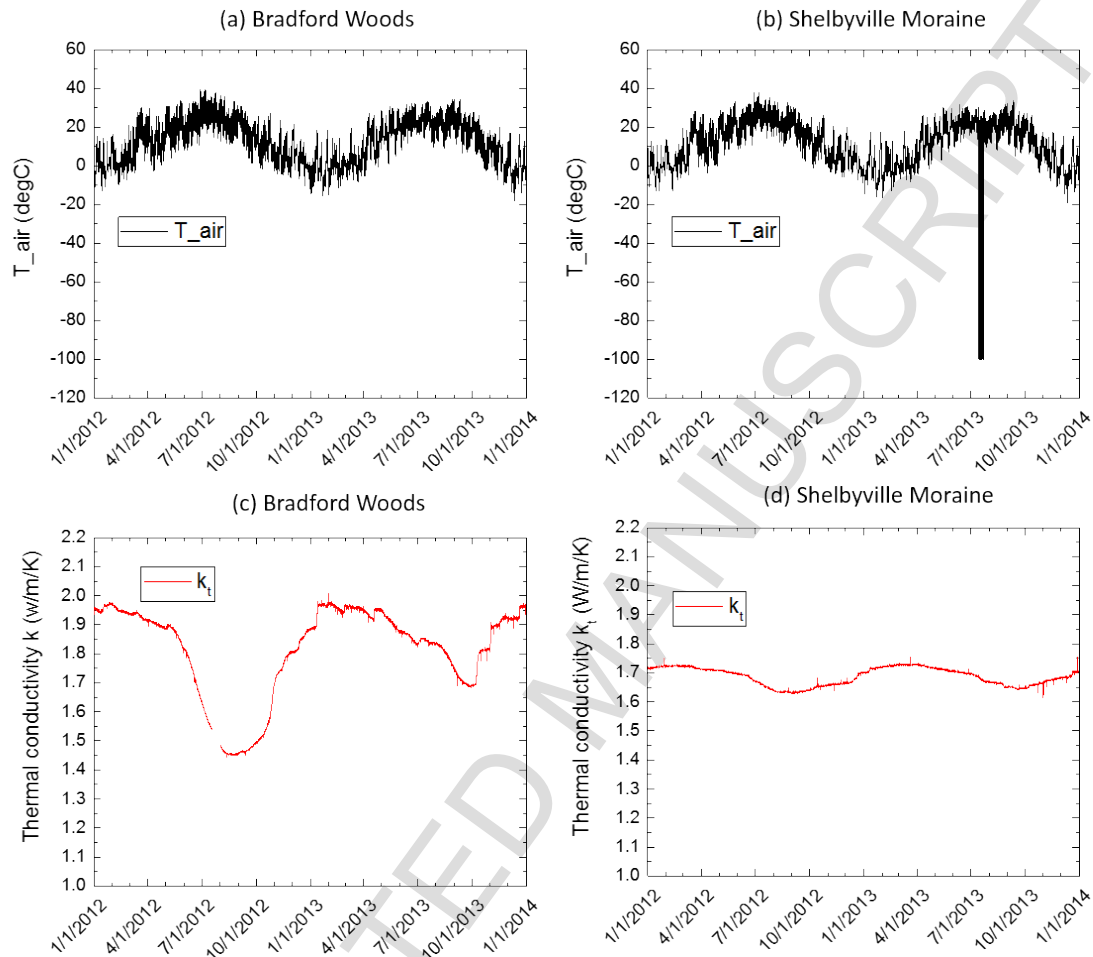


132

133 **Fig. 1.** Variation of soil temperatures at different depth (Bradford Woods (B) and Shelbyville Moraine (S))

134 Fig. 2 shows the variations of ambient air temperatures and soil thermal conductivities during 2012-2013.
 135 According to Fig. 2, the air temperatures in Bradford Woods and Shelbyville Moraine are similar, whereas

136 their thermal conductivities exhibit very different seasonal behaviors. The spikes presented in Fig. 2(b) is
 137 caused due to malfunction of the temperature sensor, which recovers to the normal level after replacement.
 138 The thermal conductivity of Bradford Woods experienced appreciable amount of decreases during the 2012
 139 water year (10/2011-09/2012) due to the decrease of soil moisture content in the drought season. [23]



140

141 **Fig. 2.** In-situ measured parameters: air temperature (a) in Bradford Woods; (b) in Shelbyville Moraine and thermal
 142 conductivity (c) in Bradford Woods; (d) in Shelbyville Moraine

143 2.2 Behaviors of horizontal GCHP system

144 2.2.1 Short-term performance of horizontal GCHP system with different configurations and 145 geological conditions

146 The short term performance of horizontal GCHP is evaluated based on its performance in ground heat
 147 extraction. The conceptual simplified model for comparison is shown in Fig. 3, the inlet temperature of the
 148 short-term performance simulation model is assigned to be a constant value of 0 °C and the corresponding
 149 outlet temperature is selected as an indicator of the horizontal GCHP system in ground heat extraction.
 150 Comparison analyses are conducted to evaluate the performance of horizontal GCHP system installed under
 151 six typical design configurations. Fig. 4 displays the geometry of those horizontal GHE configurations,

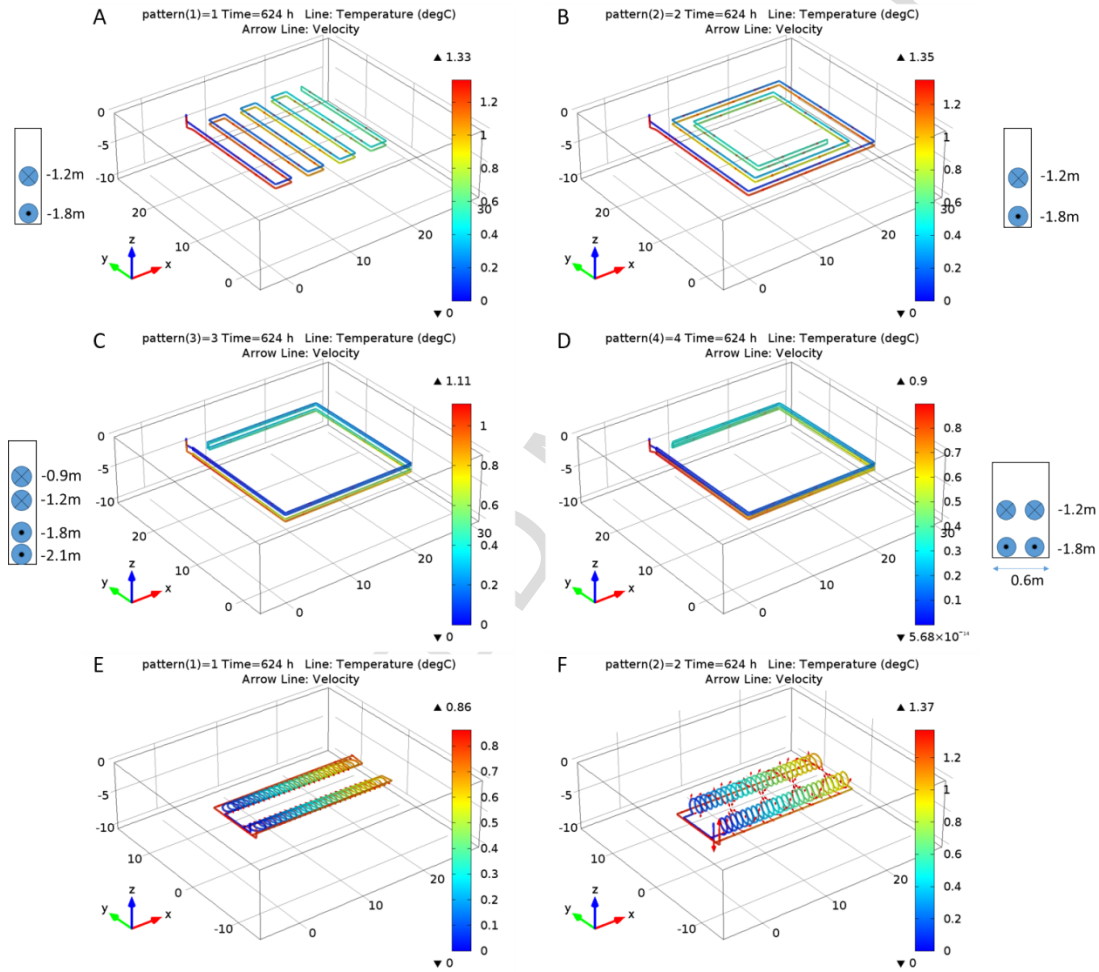
152 which generally can be classified into three types: linear GHE (A-D), slinky GHE (E) and helical GHE (F)
 153 [13]. For linear GHE, total four patterns with either two pipes per trench (A, B) or four pipes per trench (C,
 154 D) are studied, and all of them follow the recommendation proposed by ASHRAE [24].



155

156

Fig. 3. Flow chart for the short-term performance of horizontal GCHP model



157

158

159

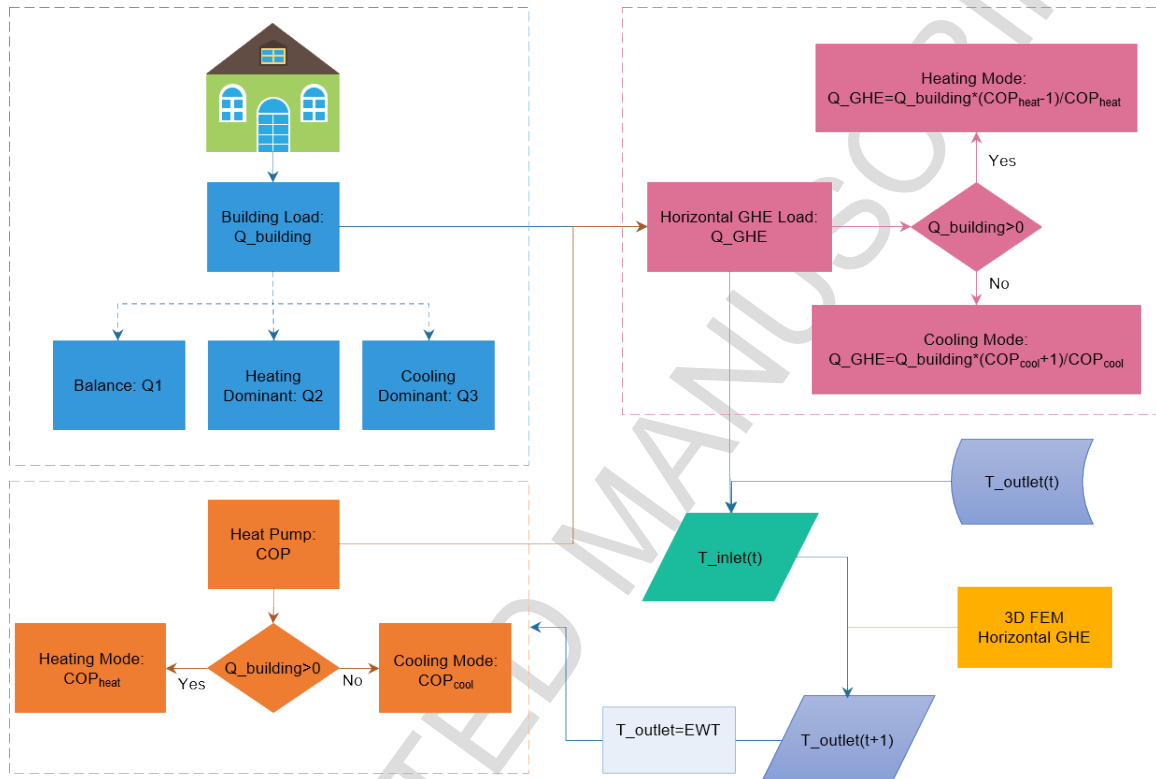
Fig. 4. Geometry of different horizontal GHE design with illustration of the temperature variation along the heat exchanger pipe in heating mode

160

161

2.2.2 Annual performance of horizontal GCHP system under different geological design conditions

162 The annual performance of the horizontal GCHP system is evaluated based on its behaviors with
 163 integration of the building loads. Three typical building load scenarios are considered including seasonal
 164 balance, heating dominant, and cooling dominant. It is assumed that the horizontal GCHP system provides
 165 sufficient capacity for building heating and cooling demand, which is estimated with a simplified building
 166 load model and heat pump operating performance curve. The annual performance of horizontal GCHP
 167 system is described by the shift of ground baseline temperature due to the annual operation of GCHP system.
 168 Different geological conditions are considered including those with relatively constant ground thermal
 169 properties versus those vary through the seasons, which are determined based on field monitoring data. Fig.
 170 5 presents the detailed flow chart for the evaluation of the annual performance of horizontal GCHP model.

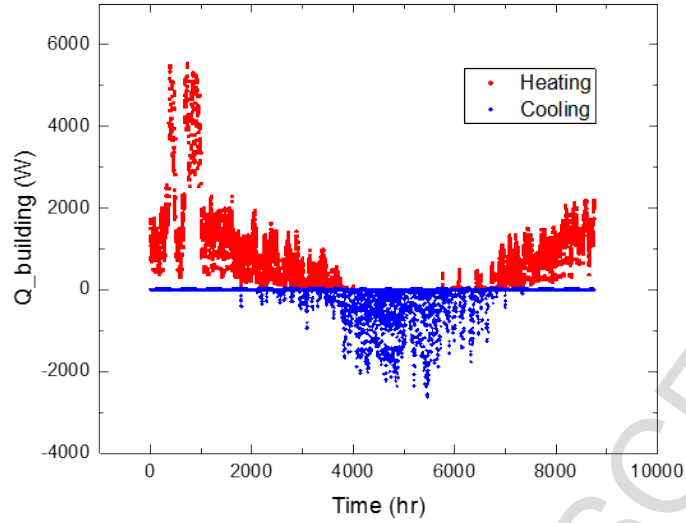


171

172

Fig. 3. Flow chart for the annual performance of horizontal GCHP model

173 Accurate description of building load can be estimated via verified code. For example, Fig.6 presents an
 174 example of the typical building load process over one-year period simulated by eQuest for a typical
 175 residential building located in Indiana with 2500 m² occupancy area. Overall, the trend of building thermal
 176 load variation can be described by a sinusoidal process, with the exception of a few periods during winter
 177 with abnormal weather conditions. The average magnitude of the sinusoidal process is close to zero, which
 178 means that the type of building load demand achieves seasonal balance approximately.



179

180 **Fig. 6.** Simulated building load process for a residential building in Indiana by eQuest (from the beginning of year)

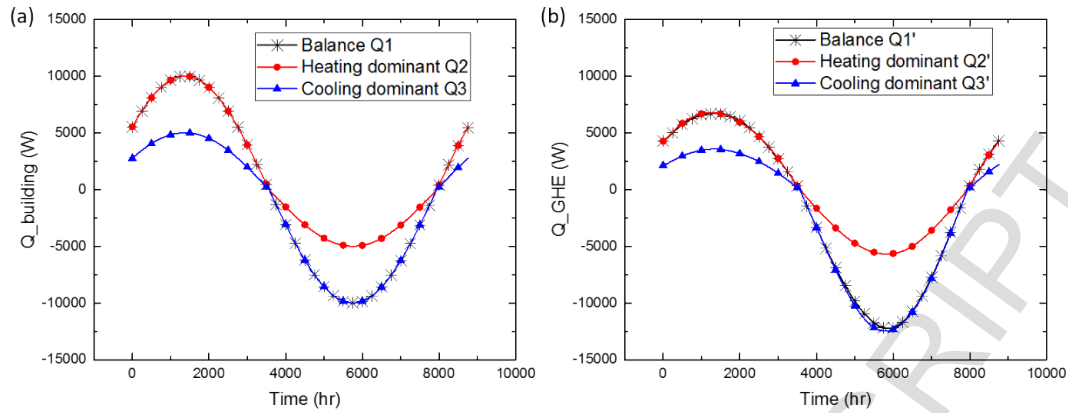
181 To simplify the analyses without incurring significant error, the building load is approximated with
 182 sinusoidal model based on the observed trend of eQuest model. The advantage of the simplified model is to
 183 make it easy to consider different building load scenarios, including seasonal balance, heating dominant, and
 184 cooling dominant. Without losing the generality, three different building loads are assumed to follow the
 185 following modified sinusoidal functions [25]:

186 Seasonal balance: $Q_1 = A * \sin(\omega t)$ (2)

187 Heating dominant: $Q_2 = 0.75A * \sin(\omega t) + 0.25A * |\sin(\omega t)|$ (3)

188 Cooling dominant: $Q_3 = 0.75A * \sin(\omega t) - 0.25A * |\sin(\omega t)|$ (4)

189 where, ω is the angular frequency, and it can be obtained by: $2\pi/T$ ($T=1$ year= $31,536,000$ s). A denotes to
 190 the peak building load which is assumed to be 10 kW in this analyses.



191

192

Fig. 7. (a) Building load profiles; (b) Source (ground) load profiles.

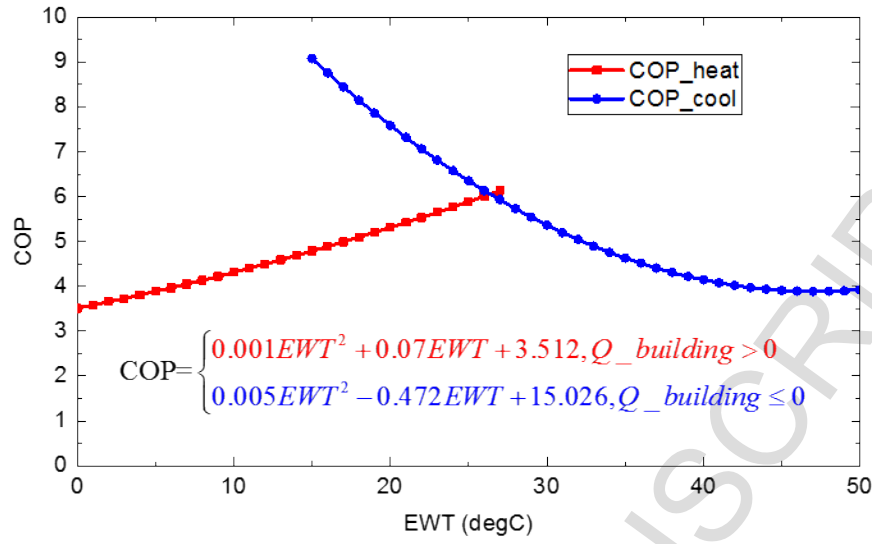
193 Fig. 7(a) shows the graphs of corresponding building loads. This simplified building load model is on the
 194 basis of two assumptions: (1) heating season ($Q_{\text{building}} > 0$) occurs before cooling season ($Q_{\text{building}} < 0$);
 195 (2) heating and cooling periods are equal throughout the year, which ignores the transition seasons (i.e.,
 196 spring, autumn) with typical $Q_{\text{building}} = 0$.

197 The performance of heat pump is typically estimated via its COP that is defined as the ratio of utilized
 198 thermal energy to electricity energy consumed for heat pump operation. The required heat injection or
 199 extraction by the GHE to meet the required building load can therefore be calculated by:

$$Q_{\text{GHE}} = \begin{cases} Q_{\text{building}} * \frac{COP_{\text{heat}} - 1}{COP_{\text{heat}}}, & Q_{\text{building}} > 0 \\ Q_{\text{building}} * \frac{COP_{\text{cool}} + 1}{COP_{\text{cool}}}, & Q_{\text{building}} \leq 0 \end{cases} \quad (5)$$

200

201 The COP is related to the Entering Water Temperature (EWT) from heat source. The dependency of COP
 202 on EWT has been documented by Shiba et al. [26], accordingly, Nam et al. [27] proposed the COP as function
 203 of EWT (in Fig. 8) when the typical design of the heat pump outlet temperature to room is 45 °C in heating
 204 mode and 7 °C in cooling mode.



205

206

Fig. 4. Performance of Heat pump versus EWT

207

The inlet temperature of GHE can be calculated by:

$$T_{\text{inlet}}(t) = T_{\text{outlet}}(t) - \frac{Q_{\text{GHE}}}{Cp_{\text{fluid}} * \rho_{\text{fluid}} * Q_v} \quad (6)$$

208

209

where the T_{outlet} is assigned to be soil temperature at $t=0$. Regardless of the heat loss between GHE outlet and heat pump inlet, the outlet temperature of GHE should be same as EWT. Then for a specific inlet temperature, the 3D FEM model for the horizontal GCHP will compute the corresponding outlet temperature at the next time step, which is then used to calculate the inlet temperature as well as the new COP at the next time step. This closed loop procedure integrates building load model with 3D FEM model for the horizontal GCHP. From these, it determines the annual performance of horizontal GCHP system.

210

211

212

213

214

215

216

217

218

219

220

221

222

223

224

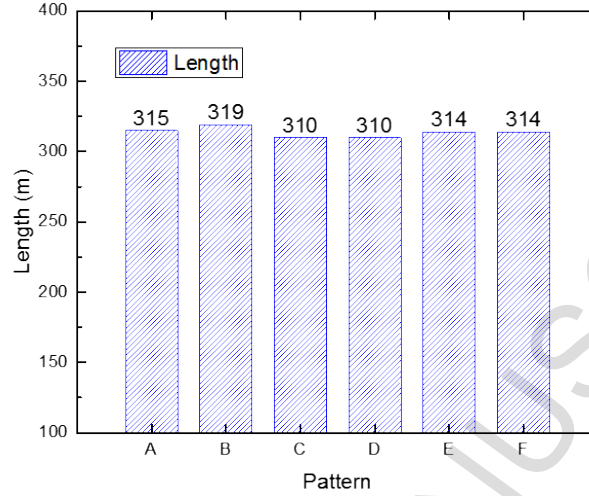
225

3. Results and discussions

3.1 Comparison of the short-term heat extraction performance of horizontal GCHP with different design configurations

The short-term performance of GCHP in different design configurations in heat extraction are simulated and discussed in this section. Fig. 9 compares the total length of GHE in different configurations, which gives an average length of 313 m. The maximum difference in the length of GHE is 9 m or around 3% of the average length. Therefore, it is assumed that the performance of GCHP design configurations are comparable based on similar total lengths. As illustrated in Fig. 4, temperature of circulation fluid increases along the heat exchange pipe for all configurations due to the thermal energy absorption from ground in heating mode. Simulations are conducted to determine the outlet temperature from GHE over 48 hours'

226 continuous operation during the coolest period of the year (Jan. 24th to Jan. 26th, 2012). The resultant
 227 temperature at the outlet after different operational times are shown in Fig. 10. The differences in the
 228 circulation fluid at the outlet shows the different performance of the GHE configuration in thermal energy
 229 extraction.



230

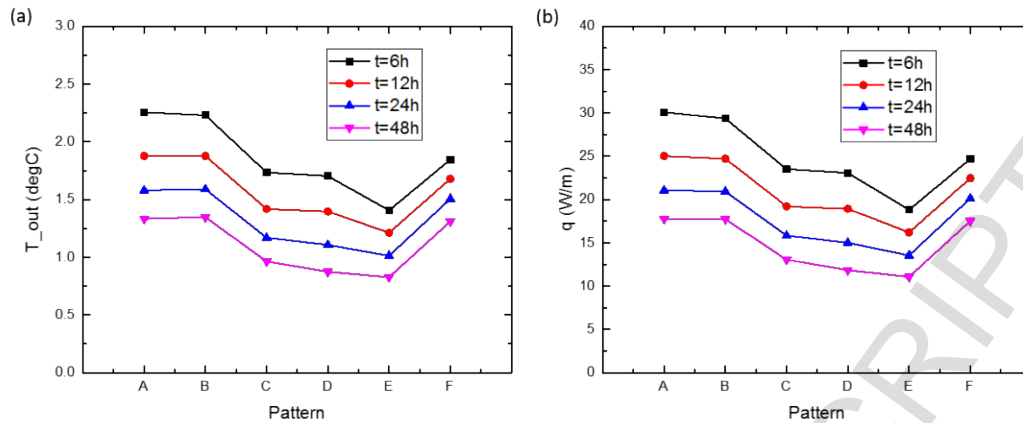
231

Fig. 9. Total installation GHE length in different configurations

232 The linear GHEs with two pipes per trench (A, B) and helical GHE (F) appear to achieve higher outlet
 233 temperature, followed by design with four pipes per trench (C, D) (Fig. 10(a)). To consider the effects of
 234 GHE length, the extracted thermal energy per length (q) is calculated as:

$$235 \quad q = \frac{Q_{GHE}}{L} = \frac{Cp_{fluid} \cdot u \cdot A \cdot \rho_{fluid} \cdot (T_{outlet} - T_{inlet})}{L} \quad (7)$$

236 in which, Q_{GHE} denotes to the total extracted thermal energy that only depends upon the outlet
 237 temperature. The results of relative performance by the per unit length thermal energy extraction showed in
 238 Fig. 10(b) are consistence with that in Fig. 10(a). In general, the GHE in configurations of A, B and F perform
 239 better in thermal energy extraction for the same installation area and similar total length. The configurations
 240 of C, D perform slightly better than E. Overall, the GHE pipe patterned in two per trench and helical shape
 241 achieved better performance in thermal energy extraction. This observation implies that the separation
 242 distance of GHE pipes has predominant effects on the efficiency of horizontal GCHP system. Smaller
 243 separation distance will lead to the less amount of energy extraction. Therefore, it is important to optimize
 244 GHE configuration to ensure the horizontal GCHP system performance, which might also need to consider
 245 factors such as installation cost. Gradual drop of thermal energy extraction is observed as the operation time
 246 goes on, which is caused by the thermal buildup effects of the adjacent ground. For example, the per unit
 247 length energy extraction, q (A), is reduced by around 40% between 6 hour of operation to 48 hour of
 248 operation. This observation is consistent with the field observation that the continuous operation negatively
 249 affects the energy extraction efficiency. Therefore, operational strategies, such as the use of intermittent
 250 operation mode, could improve the soil thermal recovery to achieve better GCHP performance.



251

252 **Fig. 10.** Comparison of heat extraction performance of different GHE configurations after different time of operation
 253 (a) the outlet temperature and (b) the energy extraction per length (GHE type A: linear zigzag with two pipes per
 254 trench, type B: linear spiral with two pipes per trench, type C: linear with four pipes per trench that are in one vertical
 255 line, type D: linear with four pipes per trench that are in two vertical lines, type E: slinky GHE and type F: helical)

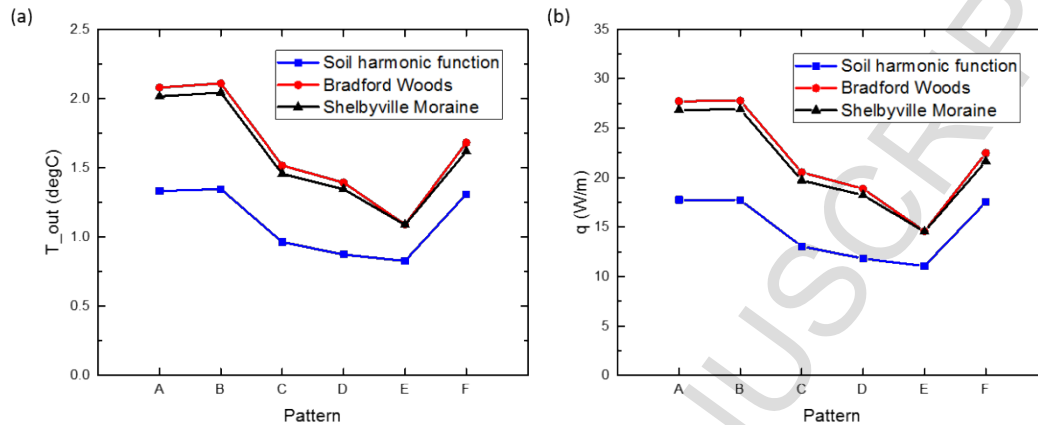
256 3.2 Influence of local geological conditions on the short-term performance of horizontal GCHP 257 system

258 The design of horizontal GCHP system requires the information about ground subsurface temperature
 259 and thermal properties of soils. The conventional design method for horizontal GCHP system generally uses
 260 the soil temperature harmonic function to describe the temperature process underground and assumes
 261 constant underground soil thermal properties. However, the influence of local geological conditions,
 262 including the seasonal variations of soil thermal properties may have significant effects on the performance
 263 of the horizontal GCHP system. To elucidate the influence of local geological conditions, analyses are
 264 conducted based on modeling each type of horizontal GCHP system subjected to three different situations:
 265 (a) underground temperature described with soil harmonic function, and soil properties are assumed to be
 266 constant at the values of the monitored average soil thermal parameters; (b) underground temperature based
 267 on in-situ measurement and use soil thermal parameters with significant seasonal variation as measured at
 268 Bradford Woods site; (c) underground temperature based on in-situ measured soil temperatures and soil
 269 thermal parameters do not show significant seasonal variations as observed in Shelbyville Moraine site.

270 The results of outlet temperature and per unit length heat extraction by different horizontal GCHP designs
 271 after 48 hours of continuous operation are summarized in Fig. 11. Evidently, the GCHPs are predicted to
 272 achieve better performance by use of field measured data compared with simplified assumptions commonly
 273 used in the current horizontal GCHP design (estimate the ground temperature for a certain region and use
 274 estimated thermal properties for soils), and the observation is true for all GCHP design configurations. This
 275 suggests that use of field data might help to mitigate the overdesign commonly found with the current
 276 horizontal GCHP system. This is a veridiction that accurate site thermal characterization can lead to cost
 277 saving for horizontal GCHP, which helps to overcome a major barrier for the use of horizontal GCHP in
 278 practice.

279 Another observation is that the performance of GCHP is only slightly better at Bradford Woods site,
 280 which has significant season variations, than that at the Shelbyville Moraine site, which has relatively stable
 281 subsurface soil properties. This might be due to the fact that the model prediction is only for short term 48

282 hours' continuous operation period, where the temporal variations in the subsurface temperature and thermal
 283 properties are insignificant. It is expected that the influence of local geological characteristics, i.e.,
 284 subsurface temperature and seasonal variations of soil thermal properties, can have a major influence on the
 285 performance of horizontal GCHP system. By applying in-situ measured soil properties, the design length of
 286 horizontal GHE can be reduced by 25% to 60% for different configurations. To this end, efforts in collecting
 287 field data should help to institute more economic design of horizontal GCHP system.



288

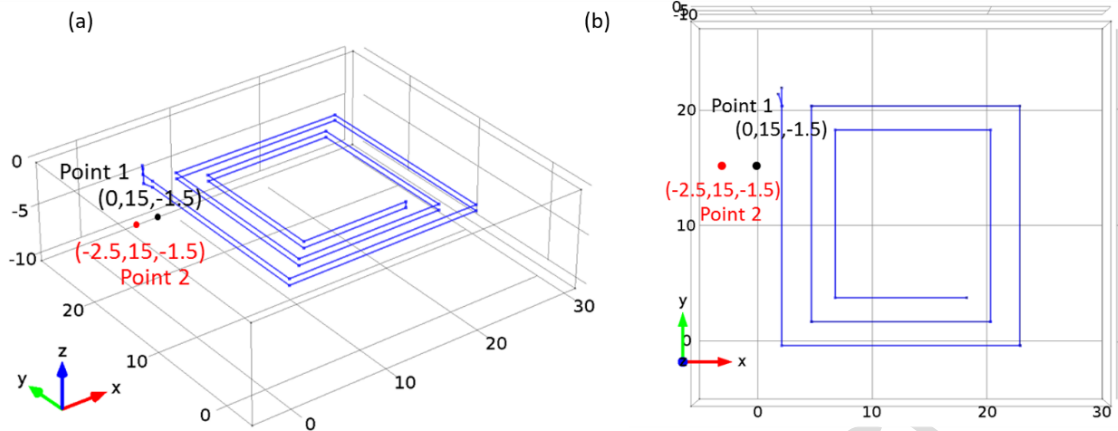
289 **Fig. 11.** (a) The outlet temperature and (b) energy extraction rate per length of horizontal GCHP system with different
 290 installation configurations at $t=48h$

291

292 3.3 Influence of local geological conditions on the annual performance of horizontal GCHP system 293 for building with balanced load

294 The influence of local geological conditions, i.e, the subsurface soil temperatures and thermal properties'
 295 seasonal variations, on the long term performance of horizontal GCHP system design is analyzed using the
 296 computational model and field data. The model considers the type B GHE design integrated with building
 297 loads as describe in section 2.2.2, and only building with seasonal balance load scenario is discussed in this
 298 part. Keep in mind, however, that for building with seasonal balanced load, due to differences in the COP of
 299 horizontal GCHP system working at heat injection or extraction modes, horizontal GCHP system injects
 300 more heat into the ground than the heat it extracts from the ground over one-year period (Fig. 7b). This could
 301 lead to thermal built-up and shift of underground baseline temperature.

302 Community scale implementation of horizontal GCHP system has shown that the shift of ground baseline
 303 temperature deteriorates its annual performance. Therefore, the shift of subsurface temperature due to GCHP
 304 system operation is used as the criteria to assess the annual performance of horizontal GCHP system. For
 305 this purpose, two locations in the ground outside the GHE pipe are selected to evaluate on the effects of
 306 GCHP system operation based on their temperature variations after one year's operation. The two selected
 307 locations are both located at the average installation depth of GHE, the coordinates of these two locations are
 308 showed in Fig. 12. Different scenarios are considered based on different extent of incorporating field
 309 monitoring data.



310

311

Fig. 12. The locations of the selected two points with (a) 3D view and (b) 2D view

312

Scenario 1: the effects of incorporating field monitored soil thermal properties

313

314

315

316

317

318

319

320

321

322

323

324

325

To elucidate the influence of soil thermal properties' seasonal variation on the GCHP system performance, comparison simulations are conducted where the same soil temperature boundary conditions based on soil harmonic function are applied. Soil thermal properties are based on in-situ monitored Bradford Woods' soil thermal properties or those using yearly average soil thermal properties. The initial inlet temperature is set to be the same and the initial soil temperature is set to be 6°C. The results of ground temperature shift at selected points 1 and 2 are shown in Fig. 13. Overall after one year's operation, the temperatures of point 1 and point 2 increase for GCHP system integrated to a building with balanced load. This is consistent with the fact that more heat is injected to the ground than that extracted due to differences in the COP of GCHP system. Compared with using an average soil thermal conductivity, the use of measured soil thermal conductivity that considers its seasonal variations leads to larger shift of ground baseline temperature. This implies that the use of field monitored site specific soil thermal properties data could help to predict and therefore prevent potential problems of ground temperature shift which compromises its efficiency.

326

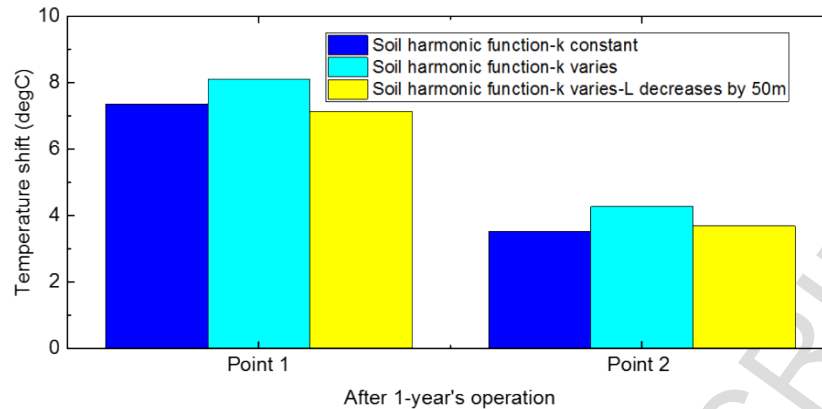
327

328

329

330

The results after the total GHE length is decreased from 319 m to 269 m, or around 15% reduction in length, are also shown in Fig. 13. By decreasing 50 m design length, the application of in-situ measured soil data shows the nearly same temperature shift as using yearly average soil data. This is sufficient to demonstrate the importance of the in-situ soil parameter measurement. With the accurate in-situ measured soil data, the optimal design of horizontal could be achieved.



331

332 **Fig. 13.** Temperature shift of point 1 and point 2 by using in-situ measured and yearly average thermal properties for
 333 building load seasonal balance scenario

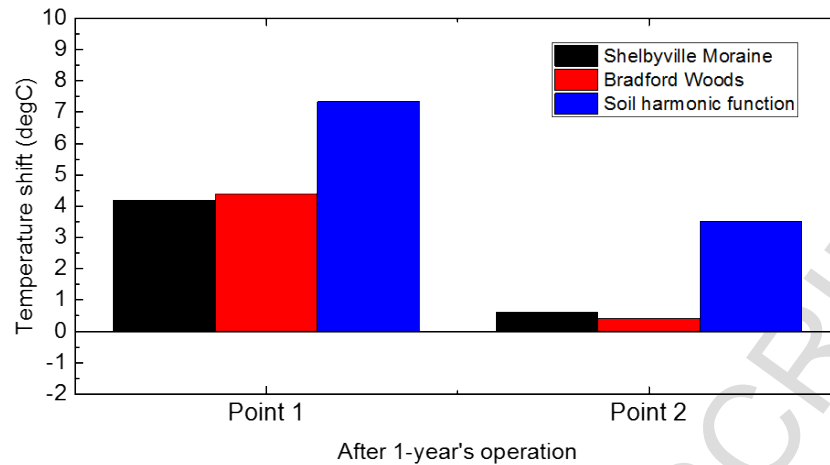
334 **Scenario 2: the effects of incorporating both field monitored subsurface temperature and soil**
 335 **thermal properties**

336 Simulation are conducted for the GCHP system after one year of service under the following design
 337 conditions: (1) underground temperature based on in-situ measurement and soil thermal parameters with
 338 significant seasonal variation as measured at Bradford Woods site; (2) underground temperature based on
 339 in-situ measured soil temperatures and soil thermal parameters do not show significant seasonal variations
 340 as observed in Shelbyville Moraine site; and (3) underground temperature described with soil harmonic
 341 function and soil properties are assumed to be constants that equal to the average value of monitored soil
 342 thermal parameters. The results of computational simulation are shown in Fig. 14. In general, the ground
 343 temperatures at both point 1 and point 2 increase after one year's operation for GCHP system integrated with
 344 a building with balanced thermal load, due to the thermal build-up effects discussed previously. Besides, a
 345 few interesting observations can be made:

346 (1) The shifts of ground temperature predicted by applying ground temperature harmonic function and
 347 constant soil thermal properties are significantly larger (around 70% increase for point 1) than those using
 348 in-situ measured ground temperature and soil thermal parameters. This implies that the application of ground
 349 temperature harmonic function as commonly used in current design will lead to overestimation of the thermal
 350 build-up effects.

351 (2) The shifts of baseline ground temperature are similar for Shelbyville, with insignificant seasonal soil
 352 thermal properties' variations, and Bradford Woods, with significant soil thermal properties' variations (Fig.
 353 14). This implies that seasonal variation of in-situ soil thermal properties does not significant affect the shift
 354 of ground temperature.

355 Incorporating the site specific subsurface temperature helps to reduce the over prediction of ground
 356 temperature shift due to imbalanced heat injection/extraction associated with GCHP system operation.



357

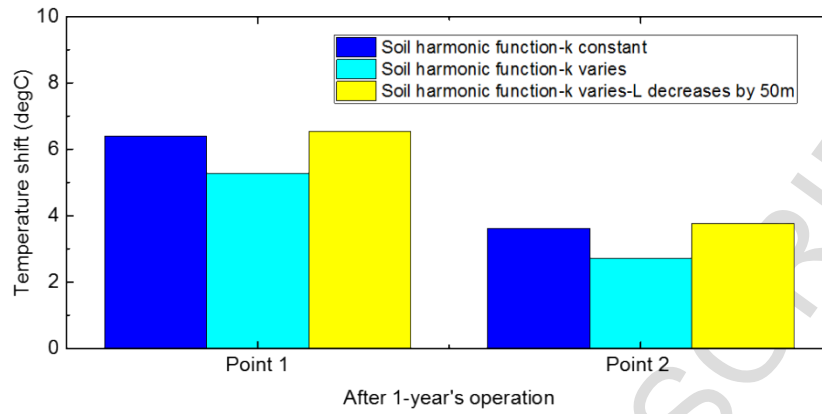
358 **Fig. 14.** Temperature shift of point 1 and point 2 after one year's operation under different geological design conditions
 359 for building load seasonal balance scenario

360 **3.4 Influence of integrated building thermal load scenarios (i.e., heating dominant or cooling**
 361 **dominant) on the annual performance of horizontal GCHP system**

362 The behaviors of GCHP system integrated with the other two types of building load scenarios, i.e., heating
 363 or cooling dominant, are also investigated. The influence of field temperature and soil thermal properties
 364 data on GCHP performance are analyzed. The results are summarized in Figs. 15-18. Fig. 15 and Fig. 16
 365 show the change of ground temperatures at selected Points 1 and 2 underground after one year of GCHP
 366 operation with integrated building that is cooling or heating dominant. The use of field monitored soil
 367 thermal properties data leads to smaller shifts of ground baseline temperature under both conditions. Fig. 17
 368 and Fig. 18 summarize the ground temperature build-up effects when both subsurface temperature and soil
 369 thermal properties are incorporated for GCHP system analyses. The comparison shows that the shift of
 370 ground temperature is less significant when GCHP system is integrated with a building that is heating
 371 dominant (i.e., in cold region). This phenomenon can be illustrated by use of Fig. 7. This is to certain extent
 372 due to the higher efficiency of heat pump working in the heating mode compared with the cooling mode.
 373 (Conceptually, the heat produced due to operation of heat pump also contributes the overall heat produced
 374 for building heating purpose.) Therefore, in the heating dominant area, although it requires providing larger
 375 amount of heat into building in the winter season than the amount of heat extracted from the building during
 376 summer season, the amount of heat actually extracted from the ground by the GHE during winter season is
 377 approximately in balance with the amount of heat injected into the ground by the GHE during the summer
 378 season. This helps to maintain balance in the heat injection and extraction. Therefore, for building load
 379 that is heating dominant, the source load (ground thermal extraction and injection) by GHE is closer to
 380 balanced heat injection/extraction from the ground. This leads to smaller thermal build-up effects under the
 381 ground. This observation indicates that stable ground temperature is more easily achieved with GCHP
 382 integrated with building that is heating dominant (or cold region). This is consistent with the documented
 383 case studies, such as a GCHP system used for residential application in heating dominant region [9], where
 384 the GCHP system did not show performance deterioration after 4 years' operation.

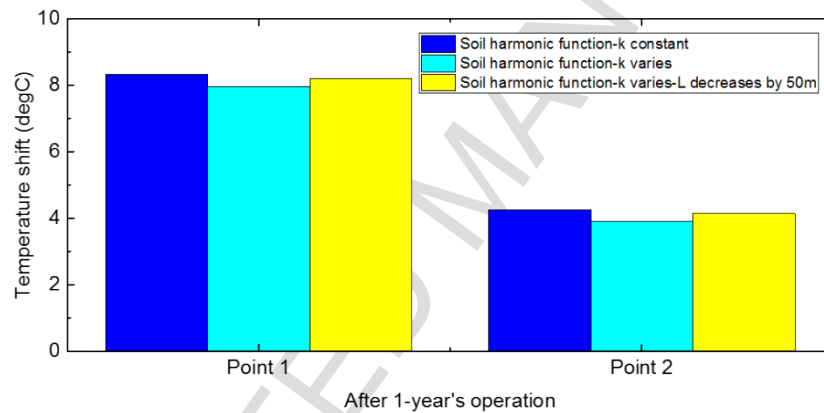
385 The analyses also show that incorporation of field monitored subsurface temperature in addition to the
 386 seasonal variation of in-situ soil properties reduces the ground temperature shift for GCHP system working

387 with building that is both heating and cooling dominant. These again validated the potential benefits of
 388 monitoring the field subsurface thermal conditions in improving the design and annual performance of GCHP
 389 system.



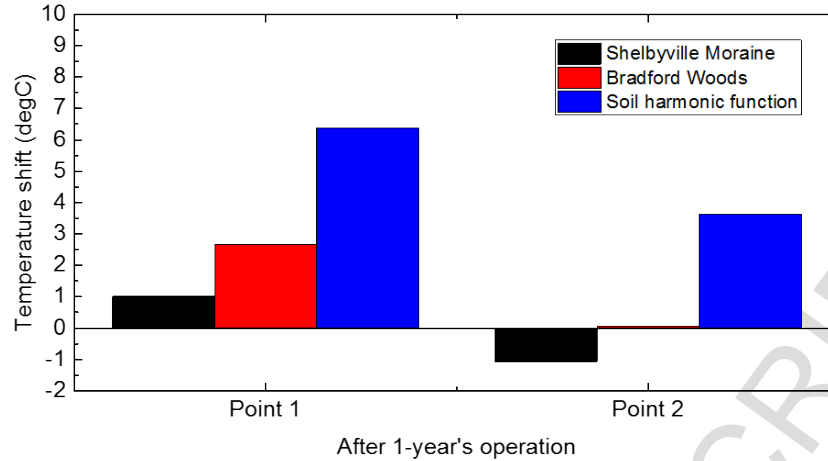
390

391 **Fig. 15.** Shift of ground temperature at point 1 and point 2 by use of in-situ measured thermal properties versus
 392 constant thermal property for GCHP integrated with a building that is heating dominant



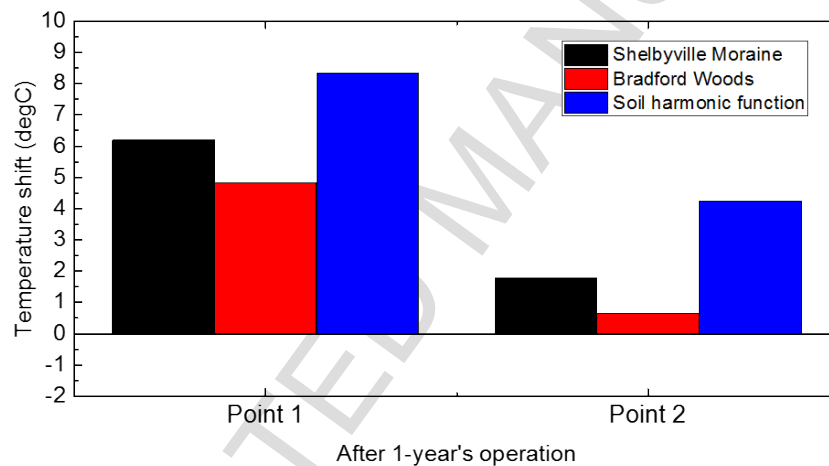
393

394 **Fig. 16.** Shift of ground temperature at point 1 and point 2 by use of in-situ measured thermal properties versus
 395 constant thermal property for GCHP integrated with a building that is cooling dominant



396

397 **Fig. 17.** Shift of ground temperature at point 1 and point 2 by use of in-situ measured ground temperature and soil
 398 thermal properties versus that assuming soil temperature harmonic function for GCHP integrated with a building that is
 399 heating dominant



400

401 **Fig. 18.** Shift of ground temperature at point 1 and point 2 by use of in-situ measured ground temperature and soil
 402 thermal properties versus that assuming soil temperature harmonic function for GCHP integrated with a building that is
 403 cooling dominant

404 4. Conclusions

405 Computational model is developed to analyze the short-term and annual performance of horizontal GCHP
 406 system. The model simulates 3D heat transfer between ground heat exchanger (GHE) and shallow ground
 407 integrated with building with different thermal loads. Major influential factors, i.e., GHE pipe patterns,
 408 geological design conditions and building load scenarios, are analyzed.

409 The short term performance of six different GHE configurations are firstly analyzed with the
 410 computational model. From these patterns of GHE layout that achieved better thermal energy exchange per

411 unit length are identified. The model predicts higher GHE performance can be achieved by using field
412 monitored temperature and thermal properties data than using estimated soil parameters as commonly done
413 in the current industry practice. It is also found that continuous operation of GCHP compromises its energy
414 extraction efficiency, which implies allowing soil thermal recovery such as by intermittent operation will
415 help the GCHP to achieve improved performance.

416 The annual performance of GCHP is evaluated by developing a model that integrates building thermal
417 load model with 3D FEM model for horizontal GHEs. With this model, three different geological design
418 conditions under three building load scenarios (i.e., balanced, heating dominant, or cooling dominant) are
419 analyzed. The shift of ground temperature is used as the indicator to compare the long term performance
420 under the assumption that the building heating/cooling demand is fully met with the GCHP system. A few
421 salient observations include:

422 1) The application of soil temperature harmonic function as design inputs will lead to the overestimation
423 of thermal build-up effects. The horizontal GCHP system is projected to achieve 25% to 60% higher
424 performance with accurate in-situ measured soil temperature data.

425 2) The seasonal variations of in-situ soil thermal properties do not show significant effects on the
426 performance of horizontal GCHP system for building with balanced thermal loads (i.e., only 0.2°C difference
427 between Shelbyville Moraine site which shows significant seasonable variation versus Bradford Woods site
428 which is relatively stable). They, however, have more appreciable effects when working with building that
429 is heating or cooling dominant (the differences between these two sites are 1.19°C and 1.37°C respectively
430 under such conditions).

431 3) Less thermal built-up occurs for horizontal GCHP system working with the building that is heating
432 dominant (or in cold region). For example, the predicted yearly temperature shift was 1.01°C for Shelbyville
433 Moraine and 2.2°C for Bradford Woods. This is possibly due to heat injection to /extraction from the ground
434 are balanced under such conditions.

435 Horizontal GCHP system features the advantages of incurring lower installation cost compared with the
436 vertical GCHP counterpart. Results of this study show that collection of field data such as subsurface
437 temperature and soil thermal properties will help to improve the prediction of its short term as well as long
438 term performance when integrated with building. This potentially will lead to 25% to 60% reduction of the
439 GHE design length, which presents an opportunity to improve the current design method in terms of cost
440 effectiveness.

441 5. Acknowledgements

442 This research is partly supported by the US National Science Foundation and China Scholarship Council.

443 6. References

- 444 [1] J. W. Lund and T. L. Boyd, "Direct utilization of geothermal energy 2015 worldwide review," in
445 *Proceedings World Geothermal Congress 2015*, Melbourne, Australia, 2015.
- 446 [2] Han and X. Yu, "Sensitivity analysis of a vertical geothermal heat pump system," *Applied Energy*, vol.
447 170, pp. 148-160, 5/15/ 2016.
- 448 [3] A. Galgaro, G. Emmi, A. Zarrella, and M. De Carli, "Possible applications of ground coupled heat
449 pumps in high geothermal gradient zones," *Energy and Buildings*, vol. 79, pp. 12-22, 8// 2014.

- 450 [4] T. Y. Ozudogru, C. G. Olgun, and A. Senol, "3D numerical modeling of vertical geothermal heat
451 exchangers," *Geothermics*, vol. 51, pp. 312-324, 7// 2014.
- 452 [5] J. Raymond and R. Therrien, "Optimizing the design of a geothermal district heating and cooling system
453 located at a flooded mine in Canada," *Hydrogeology Journal*, vol. 22, pp. 217-231, 2014.
- 454 [6] C. Rousseau, J.-L. Comlan Fannou, L. Lamarche, M. Ouzzane, and S. Kajl, "Modeling and experimental
455 validation of a transient direct expansion geothermal heat exchanger," *Geothermics*, vol. 57, pp. 95-103,
456 9// 2015.
- 457 [7] L. Pu, D. Qi, K. Li, H. Tan, and Y. Li, "Simulation study on the thermal performance of vertical U-tube
458 heat exchangers for ground source heat pump system," *Applied Thermal Engineering*, vol. 79, pp. 202-213,
459 3/25/ 2015.
- 460 [8] E.-J. Kim, M. Bernier, O. Cauret, and J.-J. Roux, "A hybrid reduced model for borehole heat exchangers
461 over different time-scales and regions," *Energy*, vol. 77, pp. 318-326, 12/1/ 2014.
- 462 [9] C. Han and X. Yu, "Performance of a residential ground source heat pump system in sedimentary rock
463 formation," *Applied Energy*, vol. 164, pp. 89-98, 2/15/ 2016.
- 464 [10] J.-L. Fannou, C. Rousseau, L. Lamarche, and K. Stanislaw, "Experimental analysis of a direct expansion
465 geothermal heat pump in heating mode," *Energy and Buildings*, vol. 75, pp. 290-300, 6// 2014.
- 466 [11] A. Buonomano, F. Calise, A. Palombo, and M. Vicidomini, "Energy and economic analysis of
467 geothermal-solar trigeneration systems: A case study for a hotel building in Ischia," *Applied Energy*,
468 vol. 138, pp. 224-241, 1/15/ 2015.
- 469 [12] Y. Shang, M. Dong, and S. Li, "Intermittent experimental study of a vertical ground source heat pump
470 system," *Applied Energy*, vol. 136, pp. 628-635, 12/31/ 2014.
- 471 [13] P. M. Congedo, G. Colangelo, and G. Starace, "CFD simulations of horizontal ground heat exchangers:
472 A comparison among different configurations," *Applied Thermal Engineering*, vol. 33-34, pp. 24-32, 2//
473 2012.
- 474 [14] S. Naylor, K. M. Ellett, and A. R. Gustin, "Spatiotemporal variability of ground thermal properties in
475 glacial sediments and implications for horizontal ground heat exchanger design," *Renewable Energy*, vol.
476 81, pp. 21-30, 9// 2015.
- 477 [15] N. Naili, M. Hazami, I. Attar, and A. Farhat, "In-field performance analysis of ground source cooling
478 system with horizontal ground heat exchanger in Tunisia," *Energy*, vol. 61, pp. 319-331, 11/1/ 2013.
- 479 [16] S. Wiryadinata, M. Modera, B. Jenkins, and K. Kornbluth, "Technical and economic feasibility of
480 unitary, horizontal ground-loop geothermal heat pumps for space conditioning in selected california
481 climate zones," *Energy and Buildings*, vol. 119, pp. 164-172, 5/1/ 2016.
- 482 [17] H. Benli, "A performance comparison between a horizontal source and a vertical source heat pump
483 systems for a greenhouse heating in the mild climate Elaziğ, Turkey," *Applied Thermal Engineering*, vol.
484 50, pp. 197-206, 1/10/ 2013.
- 485 [18] S. Sanaye and B. Niroomand, "Horizontal ground coupled heat pump: Thermal-economic modeling
486 and optimization," *Energy Conversion and Management*, vol. 51, pp. 2600-2612, 12// 2010.
- 487 [19] J. L. Casteleiro-Roca, J. L. Calvo-Rolle, M. C. Meizoso-López, A. J. Piñón-Pazos, and B. A. Rodríguez-
488 Gómez, "Bio-inspired model of ground temperature behavior on the horizontal geothermal exchanger
489 of an installation based on a heat pump," *Neurocomputing*, vol. 150, Part A, pp. 90-98, 2/20/ 2015.
- 490 [20] Z. Du and Y. Zhang, "Numerical research on the effect of Thermal Disturbance on Soil Temperature
491 Fields around wells of Vertically Buried Single-U-Tube Ground Heat Exchanger," *Journal of Convergence
492 Information Technology*, vol. 7, pp. 383-391, 2012.
- 493 [21] C. Doughty and A. Nir, Tsang, Chin-Fu, "Seasonal thermal energy storage in unsaturated soils: Model
494 development and field validation," 1991.
- 495 [22] T. Oklahoma State University. Division of Engineering and A. International Ground Source Heat
496 Pump, *Ground source heat pump residential and light commercial: design and installation guide*. Stillwater, Okla:
497 International Ground Source Heat Pump Association, Oklahoma State University, 2009.
- 498 [23] S. Naylor, S. L. Letsinger, D. L. Ficklin, K. M. Ellett, and G. A. Olyphant, "A hydrogeological approach
499 to quantifying groundwater recharge in various glacial settings of the mid-continent USA," *Hydrological
500 Processes*, vol. 30, pp. 1594-1608, 2016.
- 501 [24] ASHRAE, *ASHRAE Handbook: 2007 HVAC Applications*: American Society of Heating,
502 Refrigerating and Air-Conditioning Engineers, Inc., Atlanta, GA 30329, 2007.

- 503 [25] S. Lazzari, A. Priarone, and E. Zanchini, "Long-term performance of BHE (borehole heat exchanger)
504 fields with negligible groundwater movement," *Energy*, vol. 35, pp. 4966-4974, 12// 2010.
- 505 [26] Y. Shiba, R. Ooka, and K. Sekine, "Development of a High-Performance Water-to-Water Heat Pump
506 for Ground-Source Application," *ASHRAE Transactions*, vol. 113, pp. 261-270, 2007.
- 507 [27] Y. Nam, R. Ooka, and S. Hwang, "Development of a numerical model to predict heat exchange rates
508 for a ground-source heat pump system," *Energy and Buildings*, vol. 40, pp. 2133-2140, 2008.
- 509

ACCEPTED MANUSCRIPT

Highlights

- Developed a 3D Finite Element Model (FEM) of horizontal GCHP system integrated with building thermal loads.
- Analyzed the short term performance of different GHE configurations considering site specific geological data.
- Evaluated the long term performance of GHE integrated with different building load scenarios with consideration of monitored thermal geological data.
- Assessed the potential benefits of characterizing thermal conditions at design site to refine the design of horizontal GGHP.